

shown for  $V_{GS} = 0V$  in Fig. 1. The initial I-V for each device is given by the solid curve, while the dashed curve represents the second I-V taken in the dark. The latter corresponds to the fully collapsed I-V, where all of the traps have been filled. I-Vs taken under light illumination will appear somewhere in between the solid and dashed curves, as reflected by the amount of drain current recovery, which depends upon the amount of light applied.

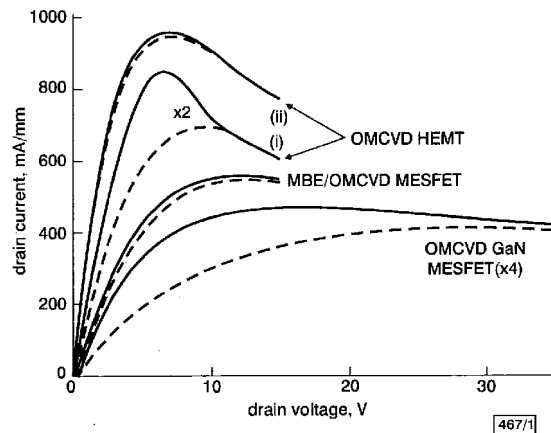


Fig. 1 Typical I-V curves for four devices studied  
Collapsed I-Vs are shown by dashed curves

The two OMCVD HEMTs in Fig. 1 ((i) and (ii)) are representative of the broad range of behaviour that we have observed from these devices, which were fabricated on materials grown under varied process conditions. The collapse in this particular MBE-grown MESFET appears much smaller than that seen in the OMCVD-grown MESFET.

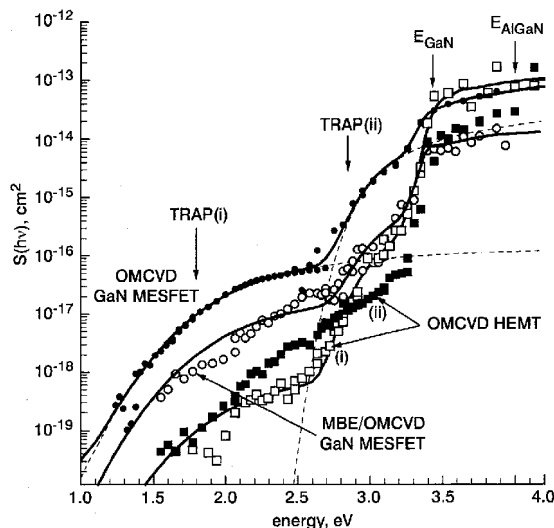


Fig. 2 Photoionisation spectra for four devices studied  
The two HEMT devices are labelled (i), (ii) to correspond to the I-V curves in Fig. 1

The photoionisation spectra of these devices,  $S(h\nu)$ , are shown in Fig. 2. The spectrum of the OMCVD MESFET was discussed in [3], and appears as the solid circles. The two broad absorptions, associated with photoionisation at two distinct traps (labelled TRAP(i) and TRAP(ii)), were identified [3] with traps in the HR GaN buffer layer. The absorptions could only be fitted (dashed lines) assuming large lattice relaxation [5], and yielded absorption thresholds at 1.8 and 2.85 eV. This identifies TRAP(i) as a mid-gap level and TRAP(ii) as a very deep acceptor/electron trap. The solid lines in the Figure are linear combinations of the fitted absorptions. The spectra of the OMCVD HEMTs (solid and open squares) and the MBE-on-OMCVD MESFET (open circles) exhibit the same spectral features as those of the OMCVD GaN MESFET, suggesting that they are due to the same traps. In addition to the trap-related absorptions, all four spectra show a clear increase at the bandgap of GaN, corresponding to the optical

excitation of free carriers. This increase is smaller in the case of the MESFETs because much of the above-gap light is absorbed in the 200 nm GaN layer that lies above the HR GaN. This, coupled with the similarity of the spectra to that of the OMCVD GaN MESFET, clearly indicates that current collapse in the HEMT devices occurs in the HR GaN layer, and that the responsible traps are identical to those in the OMCVD MESFET.

The collapse in the MBE device could be due to similar traps associated with the growth. Alternatively, if these traps are associated with dislocations, it is possible that current collapse in the MBE-grown device results from dislocations that propagate into the MBE layer from the OMCVD template. Detailed studies of MBE-grown materials are needed to better characterise the role of current collapse in these devices.

**Conclusions:** Current collapse in OMCVD-grown HEMTs has been shown to result from the same traps that produce current collapse in OMCVD GaN MESFETs. As in the MESFETs, these traps are located in the HR GaN buffer layer.

**Acknowledgments:** The authors would like to thank H.B. Dietrich and W. Kruppa for several valuable discussions. This work was supported in part by the Office of Naval Research.

© IEE 2001

11 March 2001

Electronics Letters Online No: 20010434  
DOI: 10.1049/el:20010434

P.B. Klein, S.C. Binari, K. Ikossi-Anastasiou, D.D. Koleske, R.L. Henry and D.S. Katzer (Naval Research Laboratory, 4555 Overlook Avenue SW, Washington DC 20375-5347, USA)

E-mail: klein@bloch.nrl.navy.mil

A.E. Wickenden (Army Research Laboratory, Adelphi MD 20783-1197, USA)

## References

- 1 BINARI, S.C., KRUPPA, W., DIETRICH, H.B., KELNER, G., WICKENDEN, A.E., and FREITAS, J.A., Jr.: 'Fabrication and characterization of GaN FETs', *Solid-State Electron.*, 1997, **41**, (10), pp. 1549-1554
- 2 KHAN, M.A., SHUR, M.S., CHEN, Q., and KUZNIA, J.N.: 'Current/voltage characteristic collapse in AlGaIn/GaN heterostructure insulated gate field effect transistors at high drain bias', *Electron. Lett.*, 1994, **30**, (25), pp. 2175-2176
- 3 KLEIN, P.B., FREITAS, J.A., Jr., BINARI, S.C., and WICKENDEN, A.E.: 'Observation of deep traps responsible for current collapse in GaN metal semiconductor field effect transistors', *Appl. Phys. Lett.*, 1999, **75**, (25), pp. 4016-4018
- 4 KLEIN, P.B., BINARI, S.C., FREITAS, J.A., Jr., and WICKENDEN, A.E.: 'Photoionization spectroscopy of traps in GaN metal semiconductor field effect transistors', *J. Appl. Phys.*, 2000, **88**, (5), pp. 2843-2852
- 5 JAROS, M.: 'Wave functions and optical cross sections associated with deep centers in semiconductors', *Phys. Rev. B*, 1977, **16**, (8), pp. 3694-3706

## Constrained VQ codebook design for noisy channels

Wen-Whei Chang and Heng-Iang Hsu

A codebook design approach for constrained vector quantisation using the Hadamard transform of channel transition probabilities is proposed. It is examined for quantisation of Gauss-Markov sources over channels with memory and compared with the generalised Lloyd algorithm.

**Introduction:** Vector quantisation (VQ) is an efficient speech and image compression method. However, transmitting VQ data over noisy channels changes the index bits and consequently leads to severe distortions in the reconstructed output. Forward error control could be used to protect VQ data, but it would be more efficient to design a VQ codebook with inherent good channel robustness properties. Among many design approaches to be con-

sidered [1, 2], constrained VQ codebooks given by a linear mapping of a block code (LMBC) [1] are particularly attractive in that there exists an explicit correspondence between the codewectors and the index bits transmitted on the channel. The usefulness of the LMBC-VQ may be restricted because it was originally derived for the memoryless binary symmetric channels. But transmission errors encountered in most real communication channels exhibit various degrees of statistical dependencies. It is therefore believed that further improvement can be realised through a more precise characterisation of the channel on which the codebook design is based.

*Average distortion:* The central component of a VQ system is a codebook consisting of  $M = 2^n$  codewectors with dimension  $d$ . The VQ encoder searches through the codebook for the codewector  $\mathbf{c}_i$  that best matches the input vector  $\mathbf{x}$ , and then transmits the corresponding index  $i$  to the decoder in binary format. Here, the index  $i$  is regarded as an integer representing the decimal equivalent of a binary codeword,  $\mathbf{b}(i) = (b_{m-1}(i), b_{m-2}(i), \dots, b_0(i))$ . Commonly, the input  $\mathbf{b}(i)$  and output  $\mathbf{b}(j)$  of a channel differ in the presence of an error pattern  $\mathbf{b}(e)$ . Let  $\|\mathbf{c}_i - \mathbf{c}_j\|^2$  represent the squared error distortion and let  $P(\mathbf{b}(e))$  represent the probability of receiving the index  $j$  given that the transmitted index is  $i$ . The overall distortion  $D = E[\|\mathbf{x} - \mathbf{c}_j\|^2]$  can be viewed as the sum of quantiser distortion  $D_q = E[\|\mathbf{x} - \mathbf{c}_j\|^2]$  and channel distortion  $D_c = E[\|\mathbf{c}_i - \mathbf{c}_j\|^2]$ . Following Hagen [1], an LMBC codebook can be formulated by applying a mapping matrix  $\mathbf{T}$  on a vector  $\mathbf{g}_i$  to produce its codewector  $\mathbf{c}_i$ , i.e.

$$\mathbf{c}_i = \mathbf{T} \cdot \mathbf{g}_i = \mathbf{t}_0 + \sum_{l=1}^n \mathbf{t}_l \cdot g_{i,l} \quad 0 \leq i \leq M-1 \quad (1)$$

where  $\mathbf{t}_l$  denotes column  $l$  of  $\mathbf{T}$  and  $\mathbf{g}_i = (1, g_{i,1}, \dots, g_{i,n})$  is chosen from a block code of length  $n$ . The degree of channel robustness heavily depends on the arrangements for the selecting of block code. A unconstrained VQ employs a block code with maximum codeword length  $n = M-1$ , whereas a constrained VQ incorporates only a subset of block code components. For unconstrained VQ, it was observed in [1] that  $\mathbf{g}_i = \mathbf{h}_i$ , representing column  $i$  of a Sylvester-style Hadamard matrix with elements  $\{h_{i,l}\}$ . Assuming that all the codewectors are equiprobable, the channel distortion is expressed as

$$\begin{aligned} D_c &= \frac{1}{M} \sum_{i=0}^{M-1} \sum_{j=0}^{M-1} P(\mathbf{b}(e)) \|\mathbf{c}_i - \mathbf{c}_j\|^2 \\ &= 2 \cdot \sum_{l=1}^{M-1} (1 - Q[\mathbf{b}(l)]) \|\mathbf{t}_l\|^2 \end{aligned} \quad (2)$$

where  $\|\mathbf{t}_l\|^2$  is the norm of  $\mathbf{t}_l$  and  $Q[\mathbf{b}(l)] = \sum_{e=0}^{M-1} P(\mathbf{b}(e)) h_{e,l}$  can be viewed as the scalar Hadamard transform of channel transition probabilities  $P(\mathbf{b}(e))$ . It is readily understood from eqn. 2 that for low  $D_c$ , we must ensure the mapping is such that high  $Q[\mathbf{b}(l)]$  corresponds to high-norm  $\mathbf{t}_l$  vectors, as they make a large contribution to the channel distortion.

*Block code selection:* Compared with unconstrained VQ, constrained VQ codebooks are more appropriate where complexity and channel robustness are primary considerations. Design of a constrained VQ codebook involves selecting a good block code as well as an optimisation of the mapping matrix for that specific block code. Its codewectors are

$$\mathbf{c}_i = \mathbf{t}_0 + \sum_{l \in C_B} \mathbf{t}_l \cdot d_{i,l} \quad (3)$$

where  $C_B$  specifies the set of block code components from which the codebook is generated. For memoryless binary symmetric channels, it suffices to select short block codes incorporating only components with low Hamming weights [1]. But for channels with memory, a reasonable practice is to select block code components associated with high  $Q[\mathbf{b}(l)]$  instead of those with low Hamming weights. In addition, it can be shown that block code components are divided into  $M/2$  disjunct classes and that all elements within each class have the same value of  $Q[\mathbf{b}(l)]$ . Following this, we rank the classes by descending order of  $Q[\mathbf{b}(l)]$  and then denote  $\Omega_k$  as the class which has the  $k$ th largest value of  $Q[\mathbf{b}(l)]$ . Relevant aspects of the proposed selection scheme are summarised as follows:

- (i) Set  $k = 1$  and select  $\Omega_1$  as an initial block code  $C_B$ .
- (ii) Optimise the mapping matrix  $T$  corresponding to the block code  $C_B$ .
- (iii) If channel distortion  $D_c$  is sufficiently small, then terminate. Otherwise, set  $k = k + 1$ , update the block code by  $C_B = C_B \cup \Omega_k$  and go to step (ii).

*Mapping matrix optimisation algorithm:* To optimise the mapping matrix to a given block code, we chose to minimise the quantiser distortion directly using a genetic algorithm as an optimisation technique. The main attraction of a genetic algorithm [3] is that the given search space is explored in parallel by means of iterative modifications of a population of chromosomes. The  $d \cdot (n+1)$  elements of  $T$  define the solution and hence can be encoded into a chromosome as a list of real numbers. The fitness values of all chromosomes were ranked with respect to the inverse of quantiser distortion  $D_q$ . Crossover among the selected chromosomes then proceeded by exchanging substrings of two chromosomes between two randomly selected crossover points. After crossover, mutation was applied to each chromosome by replacing one of its genes with a random number. When 30 generations were reached, the best chromosome in the final population was taken as the optimal mapping matrix. The parameter values used for the population size, the crossover probability, and the mutation probability were empirically determined to be 50, 0.8, and 0.1, respectively.

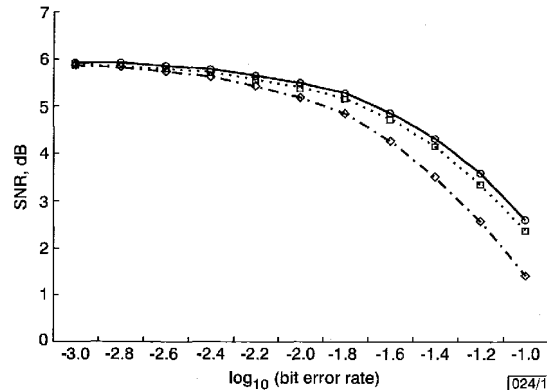


Fig. 1 SNR performance of various codebooks on Gilbert channel

- ◇ GLA
- GLA + BSA
- new algorithm

*Experimental results:* The proposed method was examined for quantisation of a first-order Gauss-Markov source, with correlation coefficient 0.5, over the Gilbert channel [4] with bit error rates ranging from  $10^{-3}$  to  $10^{-1}$ . Fig. 1 shows the SNR performances of a vector quantiser with a codebook size and vector dimension of  $(M, d) = (256, 8)$ . Our method was compared with the generalised Lloyd algorithm (GLA) [2] and GLA with binary switching algorithm (BSA) [5]. The results obtained using the proposed method clearly demonstrate an improvement over those obtained using the GLA, even with a post-processing index assignment. The investigation further showed that the improvement is more noticeable for higher bit error rates.

*Acknowledgment:* This work was supported by the National Science Council, Republic of China, under contract NSC 88-2218-E009-035.

*Conclusions:* We have explored the benefits of Hadamard transform of channel transition probabilities for use in designing a constrained VQ codebook. Experimental results indicate that the proposed method yields codebooks which more closely match the channel error statistics.

© IEE 2001  
 Electronics Letters Online No: 20010419  
 DOI: 10.1049/el:20010419

26 October 2000

Wen-Whei Chang and Heng-Iang Hsu (Department of Communication Engineering, National Chiao Tung University, Hsinchu, Taiwan, Republic of China)

E-mail: wwchang@cc.nctu.edu.tw

## References

- 1 HAGEN, R., and HEDLIN, P.: 'Robust vector quantization by a linear mapping of a block code', *IEEE Trans. Inf. Theory*, 1999, **45**, (1), pp. 200-218
- 2 LINDE, Y., BUZO, A., and GRAY, R.M.: 'An algorithm for vector quantizer design', *IEEE Trans. Commun.*, 1980, **28**, (1), pp. 84-95
- 3 GOLDBERG, D.E.: 'Genetic algorithm in search, optimization and machine learning' (Addison-Wesley, New York, 1989)
- 4 GILBERT, E.N.: 'Capacity of a burst-noise channel', *Bell Syst. Tech. J.*, 1960, **39**, pp. 1253-1265
- 5 ZEGER, K., and GERSHO, A.: 'Pseudo-Gray coding', *IEEE Trans. Commun.*, 1990, **38**, (12), pp. 2147-2158

## Efficient real-time correlator for CDMA2000 searcher

J. Kim and M. Bondarowicz

A very efficient structure for a real-time searcher in the CDMA2000 system is proposed. The advantages of using this scheme are the small amount of memory required, the processor speed per unit time, and an inherent parallel processing structure. This concept can be applied to other CDMA systems.

**Introduction:** Timing recovery, which is a combined function of searching (or initial acquisition) and tracking, is very important for the overall performance of CDMA systems, which have more than a hundred-fold faster symbol transmission rates than other wireless personal communications systems (PCSs). A searcher measures the pilot energy of possible path delays with sub-chip interval resolution, and sends them to a finger assignment logic device. The searcher needs to operate in real time to save memory and assign fingers promptly. Since this is a very high-speed process, the processors must be used efficiently. In principle, matched filtering or cross-correlation represent optimum searching methods [1]. However, they are not optimum for implementation. In this Letter, we discuss a very efficient method of designing real-time correlation circuits and describe the implementation of a searcher for a CDMA2000 base station using the proposed method.

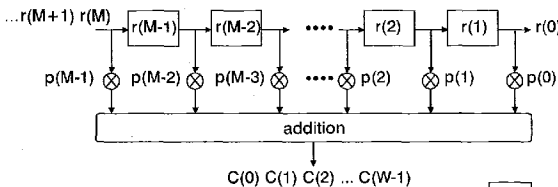


Fig. 1 Real-time correlator using matched filter

**Efficient real-time correlation:** Searching is basically a correlation process. Pilot signal samples with different time-delay hypotheses are correlated with a reference signal. The function of the correlator is defined as follows. Let the known reference sequence be  $p(i)$ .  $r(i)$ , the addition of the  $N$  time-unit delayed version of  $p(i)$  and noise  $n(i)$ , is then

$$r(i) = p(i - N) + n(i) \quad i \in \{\dots, -3, -2, -1, 0, 1, 2, 3, \dots\} \quad (1)$$

where  $i$  is a discrete time index. The correlator calculates  $C(k)$  as

$$C(k) \equiv \sum_{i=0}^{M-1} r(i+k)p(i) \quad k \in \{0, 1, 2, \dots, W-1\} \quad (2)$$

where  $M$  is the coherent integration length and  $W$  is the maximum time delay, or search window length. If  $C(K)$  is the largest of all  $\{C(0), C(1), C(2), \dots, C(K), \dots, C(W-1)\}$ , then  $K$  is the estimated time delay. From eqns. 1 and 2, we have

$$C(k) = \sum_{i=0}^{M-1} p(i+k-N)p(i) + \sum_{i=0}^{M-1} n(i+k)p(i) \quad (3)$$

The first term is the signal component and the second term is the

noise component. The signal component has its largest value when  $k$  is  $N$ . As the value of  $M$  increases, our estimation becomes more reliable.

There are several ways of implementing the correlator.  $r(i)$  can be considered as the noise-corrupted and time-delayed version of a known sequence  $p(i)$ . First, we briefly describe two conventional schemes, *store and measure* and *matched filter*, and then derive the efficient real-time correlation.

*Store and measure* is conceptually simple. Input signals are stored in memory and cross-correlated with a reference signal. If we assume that  $r(i)$  has  $B$  bits and  $p(i)$  has  $H$  bits, then we need  $(M+W)B + MH$  bits of memory. Furthermore, this is not a real-time process because the calculation will start after the arrival of the last sample  $r(M+W-1)$ . We can make this a real-time process using the *matched filter* scheme.

*Matched filter* uses an  $M$ th order finite impulse response (FIR) filter having  $p(i)$  as its coefficients, which is illustrated in Fig. 1. There is no calculation until  $r(M-1)$  arrives. There are then  $M$  multiplications and  $M-1$  additions per input sample. This scheme requires  $M \cdot (B+H)$  bits of memory. The necessary condition for real-time operation is that the processor is fast enough to support  $M$  multiplications and  $M-1$  additions per input sample period. This is not a time-efficient processor because it is active only for the last  $W$  of  $M+W-1$  sample times. For example, if the coherent integration length  $M$  is 1000 and the search window  $W$  is 100 (in general,  $M$  is much larger than  $W$  for a CDMA2000 base station), this system is active for only 9% of the time. Compared with *store and measure*, the required amount of memory is reduced by  $WB$  bits.

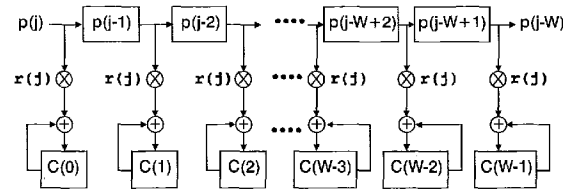


Fig. 2 Efficient real-time correlator

We propose a new real-time correlator that uniformly distributes the calculation load over time. In addition to this, our scheme requires far less memory than the previous two schemes. Our scheme is derived as follows. Let  $j = i + k$  in eqn. 2, where  $j \in \{0, 1, 2, \dots, M+W-1\}$ . Then

$$C(k) = \sum_{j=k}^{M+k-1} r(j)p(j-k) \quad k \in \{0, 1, 2, \dots, W-1\} \quad (4)$$

From eqn. 4, given input  $r(j)$ , we need  $W$  previous values of  $p(j)$ . Fig. 2 shows the implementation of this circuit. We need size  $W$  shift registers for  $p(j)$  (total memory size is  $WH$ ),  $W$  registers for  $C(k)$ , and no memory for  $r(j)$ . For each new received signal  $r(j)$ , there is a new reference signal  $p(j)$  for the shift register.  $W$  multiplication results are then accumulated in  $W$  registers. There are  $W$  multiplications and additions per input sample. In other words, the necessary condition for real-time operation is that the processor is fast enough to support  $W$  multiplications and additions per input sample period. This is a time-efficient system because there is no idle period. For example, if  $M$  is 1000 and  $W$  is 100, the required system speed for real-time operation is only 10% of the *match filter* method, which is achieved by uniformly distributing the calculation load over time. Furthermore, this scheme requires only  $WH$  bits of memory. For example, if  $H$  is 1 bit (PN codes have 1 bit values) and  $B$  is 4 bits, the required amount of memory is only 2% of that required by the *matched filter* scheme. The merits of this scheme are as follows:

- (i) No memory is required for input sample  $r(j)$ .
- (ii) Small memory size requirement for reference sample  $p(j)$ .
- (iii) Uniform distribution of calculation load over time: there is no idle time and the processor speed requirements per unit time for real-time processing are minimised.
- (iv) Inherent parallel processing structure: In Fig. 2, there is separate processing per each  $C(k)$ . We may have  $W$  separate parallel processors, or we can group multiple  $C(k)$ s and assign one faster processor.